ASIA-PACIFIC JOURNAL OF CHEMICAL ENGINEERING
Asia-Pac. J. Chem. Eng. 2010; **5**: 179–190
Published online 10 September 2009 in Wiley InterScience
(www.interscience.wiley.com) DOI:10.1002/apj.368

Curtin University of Technology

Special Theme Research Article

Solar membrane natural gas steam-reforming process: evaluation of reactor performance

M. De Falco,[1] A. Basile[2] and F. Gallucci[3]*

[1]*Chemical Engineering Department, University of Rome ''La Sapienza'', via Eudossiana 18 00184 Rome, Italy*
[2]*Institute on Membrane Technology, ITM-CNR, via P.Bucci 17/c 87030 Rende (CS), Italy*
[3]*Fundamentals of Chemical Reaction Engineering Group, Faculty of Science and Technology, University of Twente, Enschede, The Netherlands*

Received 15 December 2008; Revised 29 January 2009; Accepted 17 February 2009

ABSTRACT: In this work, the performance of an innovative plant for efficient hydrogen production using solar energy for the process heat duty requirements has been evaluated via a detailed 2D model. The steam-reforming reactor consists of a bundle of coaxial double tubes assembled in a shell. The annular section of each tube is the reaction zone in which Ni-based catalyst pellets are packed, whereas the inner tube is a dense Pd-based selective membrane that is able to remove hydrogen from the reaction zone. By coupling reaction and hydrogen separation, equilibrium constrains inside the reactor are circumvented and high methane conversions at relatively low temperatures are achieved. The heat needed for the steam-reforming reaction at this low operating temperature can be supplied by using a molten salt stream, heated up to 550 °C by a parabolic mirror solar plant, as heating fluid. The effects on membrane reactor performance of some operating conditions, as gas mixture residence time, reaction pressure and steam-to-carbon ratio, are assessed together with the enhancement of methane conversion with respect to the traditional process, evaluated in the range 40.5–130.9% at the same operating conditions. Moreover, owing to the use of a solar source for chemical process heat duty requirements, the greenhouse gases (GHG) reduction is estimated to be in the range 33–67%.

KEYWORDS: Steam reforming; membrane reactor; solar energy; hydrogen production

INTRODUCTION

The well-known energetic issue is stimulating the development of clean innovative technologies for the reduction of greenhouse gases (GHG) emissions and the creation of a more sustainable economic structure worldwide. Hydrogen goes into this context as one of the most promising new frontiers to be explored, as the energy vector of the future. In fact, hydrogen can be produced by using renewable energy sources and can be converted into fuel cells, producing electrical energy without emitting polluting substances. Moreover, deterioration of crude oil quality, more stringent petroleum product specifications and environmental problems will all lead to an increased need of hydrogen to be used in hydroprocessing.

Hydrogen can be produced by water splitting, using electrical energy or thermochemical cycles or from fossil fuels such as natural gas, carbon and heavy hydrocarbons.

**Correspondence to*: M. De Falco, Chemical Engineering Department, University of Rome "La Sapienza", via Eudossiana 18 00184 Rome, Italy. E-mail: marcello.defalco@uniromal.it

Surely, the natural gas steam-reforming process is the most important process to produce large amounts of hydrogen. It is based on the following main reactions:

$$CH_4 + H_2O \Leftrightarrow CO + 3H_2 \quad \Delta H^\circ_{298\ K} = 206\frac{kJ}{mol} \tag{1}$$

$$CO + H_2O \Leftrightarrow CO_2 + H_2 \quad \Delta H^\circ_{298\ K} = -41\frac{kJ}{mol} \tag{2}$$

$$CH_4 + 2H_2O \Leftrightarrow CO_2 + 4H_2 \quad \Delta H^\circ_{298\ K} = 165\frac{kJ}{mol} \tag{3}$$

The steam-reforming reaction (1) is highly endothermic and very fast with the Ni/Al_2O_3 catalyst. The chemical equilibrium threshold leads to operation at high temperature, therefore the conventional tubular packed bed reactors are placed in a furnace radiant chamber. A part of natural gas (methane) feedstock is burned to supply the great amount of heat duty, without producing hydrogen. For this reason, a large amount of CO_2 is emitted as reaction and combustion products: considering

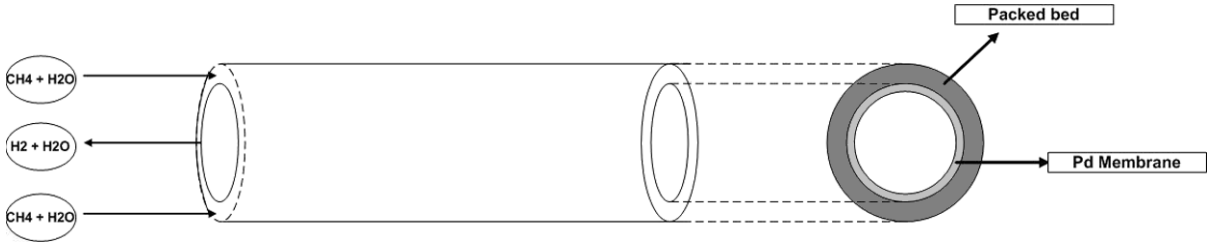

Figure 1. Steam-reforming membrane reactor draft (sweeping gas = H_2O).

that carbon dioxide emitted per unit of hydrogen produced is within the range 8.3–10.1 kg_{CO_2}/kg_{H_2}, depending on process efficiency (typically 65–80%)[1] and that 32 million tonnes of hydrogen is produced per year by the steam-reforming process, this process emits about 300 million of tonnes of CO_2 worldwide every year.

The aim of this work is to investigate an innovative solar membrane reformer that is able to improve steam-reforming process efficiency and reduce the GHG emissions drastically, owing to the harmony between two innovative technologies: the membrane reactor (MR) and concentrating solar power (CSP) plant based on molten salt.

Pd-based membrane reactor

The integration of selective membranes inside the reaction environment seems to be an interesting and applicable method to reduce the operating temperature needed to carry out the endothermic steam-reforming reaction. In fact, if a hydrogen-selective membrane is placed directly inside the reaction zone, the hydrogen produced is quickly removed, avoiding equilibrium conditions to be achieved. By this way, the NG steam reforming (1) and the WGS (2) are promoted as reaction conditions are far from equilibrium and reaction rates are fast.

In order to be applied in the reaction environment, a membrane has to own the following properties:

1. High selectivity towards a reaction product (hydrogen) that has to be recovered from the reaction environment.
2. High permeability in order to operate with high permeation flux and to reduce the membrane surface area needed.
3. Good mechanical stability to allow operation under high pressure differences, with enhanced permeation fluxes and reduced volumes of the reacting mixture. A supported membrane, composed of a thin layer (20 μm) of selective material (Pd–Ag) and a support that is able to stand up to mechanical stress, is stable under the reaction pressures range explored in this work.
4. Good chemical resistance to avoid the deterioration of the membrane during the normal operation.

Inorganic membranes seem to be promising candidates, particularly the Pd-based membranes among them, owing to their very high selectivity towards hydrogen. During the past few years, many papers have been published regarding Pd-based MRs for improvement of chemical process performance,[2–14] attesting the growing interest of the scientific and technological community.

Figure 1 shows a MR concept: the reactor is composed of two concentric tubes, whose internal is the selective membrane itself (permeation zone), while the catalyst pellets are packed in the annulus (reaction zone). As the reactions occur, the hydrogen produced is removed through the membrane and swept out by a sweeping gas or sucked by a vacuum pump. In the present work, sweep gas (water vapour) has been considered. The hydrogen is recovered in the outline of the permeation zone and separated from steam by condensation.

By this way, the operating temperature is much lower than the temperature to be reached in the traditional process (500 °C *vs* 800–900 °C)[15] as the process is not controlled by a thermodynamic equilibrium.

The catalyst pellets are packed in the annulus because in this way the membrane is far from the hot tube wall and membrane temperature is maintained at lower values, assuring a more stable operation.

Concentrating solar power molten salt plant

The CSP scheme is represented in Fig. 2 for a solar trough system with molten salts heating the carriers up to 550 °C and two-tanks molten salt storage.

The CSP plant basically consists of a solar collector field, a receiver, a heat transfer fluid loop and a heat storage system. The mirrors of the solar field concentrate the direct solar radiation on the solar receiver set at the focal line. The heat transfer fluid (e.g. molten salts) removes the high temperature solar heat from the receiver that is afterwards collected into an insulated heat storage tank to be pumped, on demand, to the heat users (steam generators, endothermic reactors,

DOI: 10.1002/apj

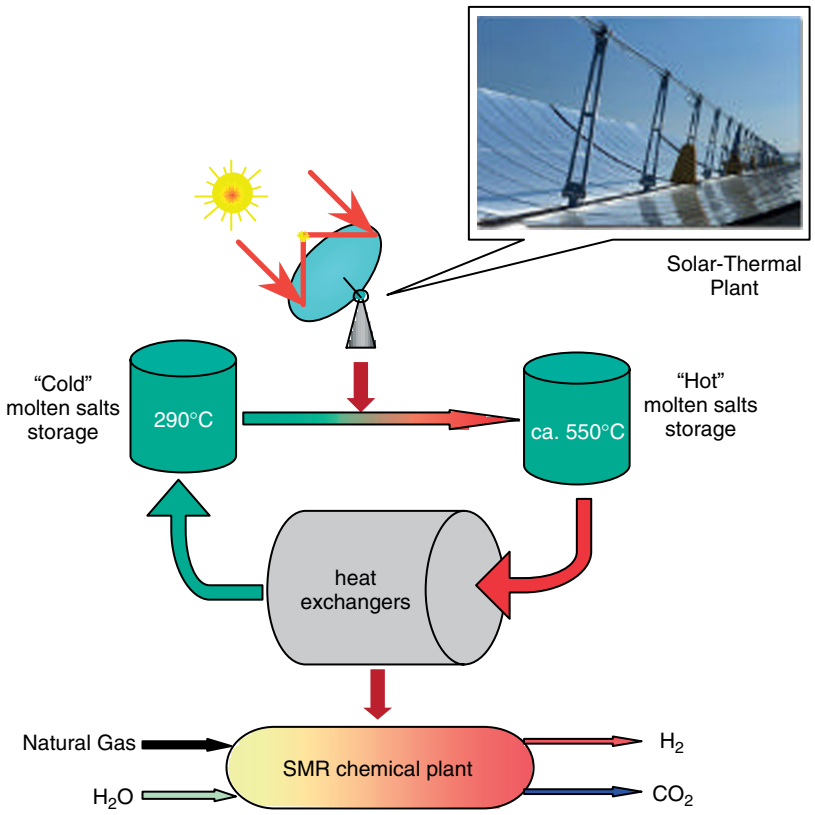

Figure 2. Simplified scheme of parabolic trough power plant with two-tank molten salt storage. This figure is available in colour online at www.apjChemEng.com.

etc.), where it releases its sensible heat. Finally, the heat carrier fluid is stored into a lower temperature tank ready to restart the solar heat collection loop.

The idea to match the CSP plant with natural gas steam-reforming MR derives from the consideration that the thermal level reached by molten salt stream (550 °C) is adherent to the thermal requirements of MR (preferred operating temperature equal to 500 °C).

PROCESS DESCRIPTION

The layout of the plant is reported in Fig.3. The reactant mixture, composed of methane and steam, is fed to the MR reaction zone, while a sweeping gas (steam) is fed to the permeation zone in order to keep the hydrogen partial pressure as low as possible and to increase the hydrogen flux through the Pd-based membrane. A molten salt stream is used as a heat carrier to supply the heat duty required by the steam-reforming reactions.

The retentate gas mixture consists of un-reacted methane and steam, hydrogen, carbon monoxide and dioxide. After the steam recovery by condensation, the outlet gas mixture has a high net heat value, which can be used to generate a medium-high pressure steam and consequently electrical energy, resulting in an increase in the overall energy efficiency.

The permeation zone outlet is a mixture of hydrogen and steam. The hydrogen is recovered by condensation, compressed and stored.

A molten salt stream is sent to process and sweeping water boilers, then the residual sensible heat (molten salt is stored in cold tank at 290 °C, as shown in Fig. 2) is used to produce electricity.

Therefore, the proposed plant is co-generative as it is able to produce both hydrogen and electricity, and it is a hybrid plant considering the simultaneous utilisation of solar source and natural gas.

Some heat recoveries are foreseen in order to reduce the heat load supplied by molten salt and consequently increase the electricity production:

- In the process steam cycle, process H_2O condensed can pass in the first section of the H_2O condenser in order to recover a part of the heat needed to be re-vaporised and fed to the reaction zone.
- In the sweeping steam cycle, sweeping H_2O condensed can pass in the first section of H_2O condenser in order to recover a part of the heat needed to be re-vaporised and fed to the permeation zone.

DOI: 10.1002/apj

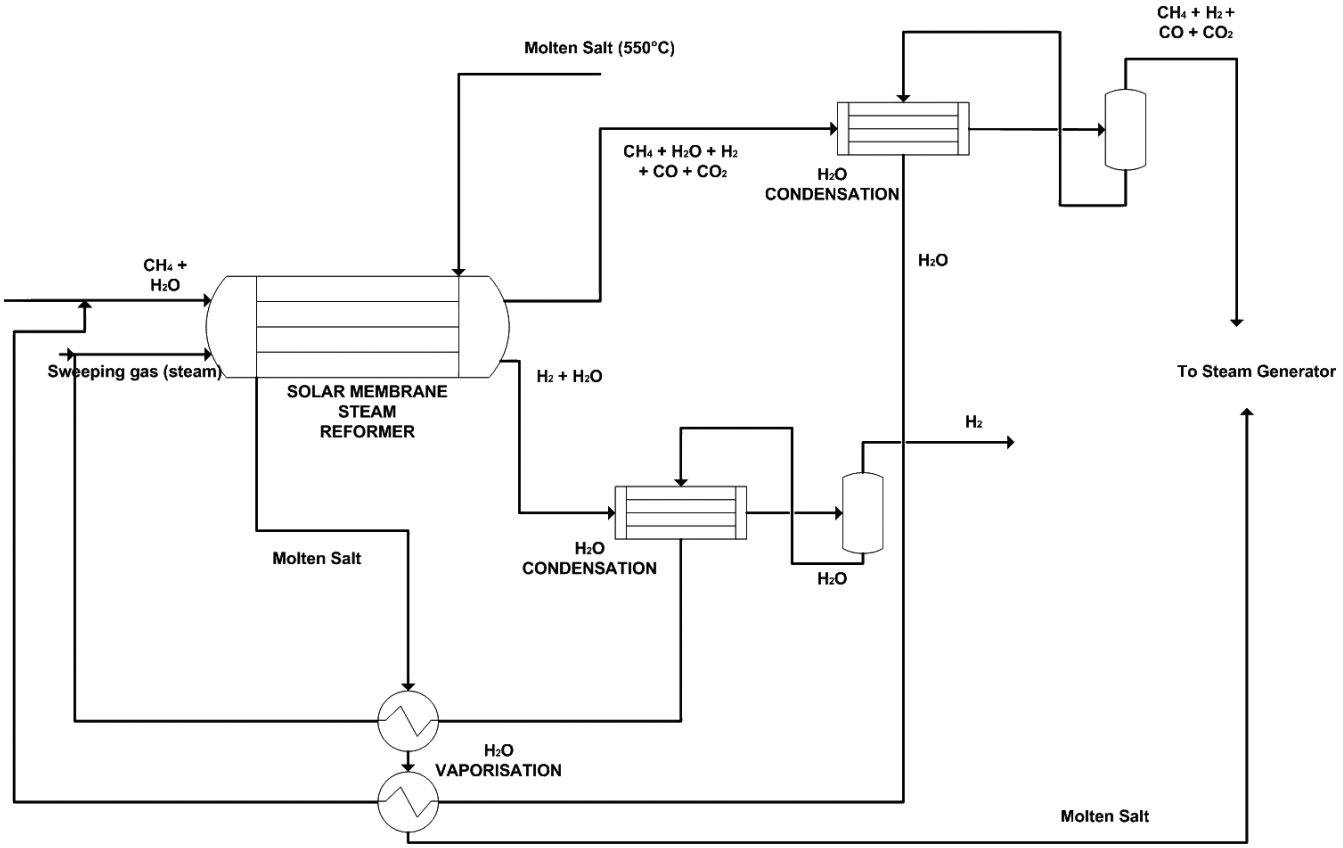

Figure 3. Process scheme layout.

Figure 4 shows the section of membrane reactor system simulated in the following. The reactor is composed of a bundle of four membrane reformers assembled in a heat exchanger, in which molten salt is fed from the shell side.

MATHEMATICAL MODEL

The reactor model is based on mass, energy and momentum balances. The two-dimensional nature of the model allows axial and radial concentrations and temperature profiles to be evaluated.

Secondary reactions other than (1–3), such as carbon coke formation, are not considered in this study.

The following assumptions are made:

- steady-state conditions;
- negligible axial dispersion and radial convective terms;
- ideal gas behaviour;
- each double tube is representative of any other tube;
- pseudo-homogenous condition inside the reactor;
- a single pseudo-effectiveness factor, independent of reaction and of local conditions;
- 100% Pd-based membrane hydrogen perm-selective.

Mass balances

Membrane reformer reaction zone

The mass balances for all the gas mixture components are as follows:

$$\frac{\partial(\tilde{u}_z\tilde{c}_i)}{\partial\tilde{z}} = \frac{d_P \cdot L}{Pe_{\mathrm{mr}} \cdot {r_{i,o}}^2} \times \left(\frac{\partial^2(\tilde{u}_z\tilde{c}_i)}{\partial\tilde{r}^2} + \frac{1}{\tilde{r}}\frac{\partial(\tilde{u}_z\tilde{c}_i)}{\partial\tilde{r}}\right) - \frac{\rho_b \cdot L}{u_{z,\mathrm{in}}c_{\mathrm{CH_4,in}}} \cdot \eta \cdot R_i \quad (4)$$

where $\tilde{u}_z$ and $\tilde{c}_i$ are the dimensionless gas mixture velocity and mole concentration of component i (CH_4, H_2O, H_2, CO and CO_2), $u_{z,\mathrm{in}}$ and $c_{\mathrm{CH_4,in}}$ are the inlet velocity and the inlet methane concentration, $\tilde{z}$ and $\tilde{r}$ are dimensionless axial and radial coordinates, d_p is the catalyst particle diameter, L and $r_{i,o}$ are the reactor length and the catalytic bed tube radius respectively, ρ_b is the packed bed density, η and R_i are the effectiveness factor and the intrinsic rate for component i, expressed according to Xu and Froment[16] kinetics scheme, based on Langmuir–Hinshelwood mechanism and $\mathrm{Pe_{mr}}$ is the mass effective radial Peclet number given by Kulkarni and Doraiswamy[17] for Reynolds number greater than 1000.

DOI: 10.1002/apj

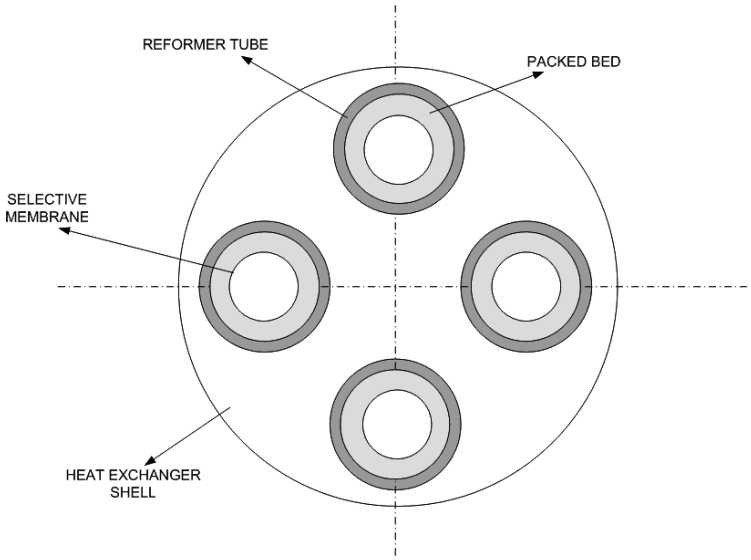

Figure 4. Four tubes-and-shell reactor configuration.

In the following, the expressions of R_i are reported for each component:

$$R_{CH_4} = -(R_1 + R_3)$$
$$R_{H_2O} = -(R_1 + R_2 + 2R_3)$$
$$R_{H_2} = 3R_1 + R_2 + 4R_3$$
$$R_{CO} = R_1 - R_2$$
$$R_{CO_2} = R_2 + R_3$$

Membrane reformer permeation zone

In the inner tube, a sweeping gas (steam) flows to carry permeated hydrogen out of the membrane module. The hydrogen mass balance gives

$$\frac{dY_{H_2}}{d\tilde{z}} = \pm\frac{N^m_{H_2} \cdot 2\pi \cdot r_{o,i}}{F_{CH_4,in}} \tag{5}$$

where Y_{H2} is the ratio between permeated hydrogen ($F_{H_2,perm}$) and inlet methane flow rate ($F_{CH_4,in}$), $r_{o,i}$ is the inner tube external radius and $N^m_{H_2}$ is the hydrogen flux permeating through the membrane, calculated according to the well-known Sieverts' law:

$$N^m_{H_2} = \frac{B_H}{\delta} \cdot (p^{0.5}_{H_2,reac} - p^{0.5}_{H_2,perm}) \tag{6}$$

In Eqn. (6), B_H is the hydrogen permeability, calculated according to Shu *et al*.[2] for Pd–Ag membranes, δ is the membrane thickness (20 μm in the following simulations) and $p_{H2,reac}$ and $p_{H2,perm}$ are the hydrogen partial pressures in reaction and permeation zones respectively.

The sign + or − in Eqn. (5) is used if the sweeping gas is fed co-current or counter-current with respect to the reactant gas mixture respectively.

Energy balances

Membrane reformer reaction zone

$$\frac{\partial\tilde{T}^R}{\partial\tilde{z}} = \frac{\lambda_{er} \cdot L}{(u_z \cdot c_{tot}) \cdot c_{p,m} \cdot {r_{i,o}}^2} \times \left(\frac{\partial^2\tilde{T}^R}{\partial\tilde{r}^2} + \frac{1}{\tilde{r}}\frac{\partial\tilde{T}^R}{\partial\tilde{r}}\right) + \frac{\rho_b \cdot L \cdot \eta \cdot \sum_{j=1}^{3}(-\Delta H_j) \cdot R_j}{T_{R,in} \cdot (u_z \cdot c_{tot}) \cdot c_{p,m}} \tag{7}$$

where $\tilde{T}_R$ and $T_{R,in}$ are the dimensionless reaction zone temperature and the inlet temperature, $c_{p,m}$ is the specific heat of gas mixture, c_{tot} is the total gas concentration, R_j is the reaction rate of reaction j ($j = 1, 3$), $(-\Delta H_j)$ is the enthalpy of reaction j and λ_{er} is the effective radial thermal conductivity of packed bed and gas mixture, considered as a pseudo-homogeneous phase and calculated according to Elnashaie and Elshishini.[1]

Membrane reformer permeation zone

$$\frac{d\tilde{T}_P}{d\tilde{z}} = \pm\frac{L}{F_{P,tot} \cdot c_{p,perm} \cdot T_{R,in}} \cdot \left[U_1 \cdot 2\pi \cdot r_{i,i} \cdot T_{R,in}\left(\tilde{T}_R - \tilde{T}_P\right) + N^m_{H_2} \cdot \pi \cdot r_{o,i} \cdot \left(h_{R,H_2} - h_{P,H_2}\right)\right] \tag{8}$$

where $\tilde{T}_P$ is the dimensionless permeation zone temperature, $F_{P,tot}$ and $c_{p,perm}$ are the total molar flow rate in the permeation zone and the permeation zone gas mixture specific heat and h_{R,H_2} and h_{P,H_2} are the reaction and permeation zone hydrogen enthalpies.

DOI: 10.1002/apj

The overall heat transfer coefficient U_1 [Eqn (8)] between reaction and permeation zone is given by

$$U_1 = \left[\frac{1}{h_W} + \frac{\delta}{\alpha_{\text{mem}}} + \frac{r_{o,i}}{r_{i,i}} \cdot \frac{1}{h_{w,p}}\right]^{-1} \tag{9}$$

where α_{mem} is the membrane thermal conductivity and $h_{w,p}$ is the heat convective transport coefficient in the permeation zone, calculated at turbulence conditions, while h_W is the heat transfer coefficient of an 'unmixed layer' near the tube wall where heat transport occurs only by molecular conduction, as reported by Tsotsas and Schlünder.[18] h_W is calculated by applying the expression reported by Li and Finlayson[19]:

$$h_W = 0.17 \cdot \frac{\lambda_g}{d_p} \cdot \left(\frac{\text{Pr}}{0.7}\right)^{\frac{1}{3}} \cdot \text{Re}^{0.79} \tag{10}$$

where λ_g is the gas mixture conductivity.

Molten salt shell

$$\frac{d\tilde{T}_{\text{MS}}}{d\tilde{z}} = \pm\frac{U \cdot L}{w_{\text{MS}} \cdot c_{p,\text{MS}}} \cdot (\tilde{T}_{\text{MS}} - \tilde{T}_R) \cdot 2\pi \cdot r_{i,o} \quad (11)$$

where $\tilde{T}_{\text{MS}}$, w_{MS} and $c_{p,\text{MS}}$ are the dimensionless temperature, the mass flow rate and the specific heat of molten salt stream.

The term U is the overall heat transfer coefficient between the heating fluid stream and the packed bed, calculated by

$$U = \left(\frac{1}{\alpha_{\text{met}}} + \frac{1}{h_W}\right)^{-1} \tag{12}$$

where α_{met} is the metal tube conductivity

In Eqn (8) and (11) the sign + or − is used depending on the sweeping gas and molten salt co-current (+) or counter-current (−) configuration. For the sake of simplicity, in the following simulations, co-current configuration is assumed for both sweeping gas and molten salt.

Momentum balances

The momentum balance is considered only in the reaction zone:

$$\frac{dP_{\text{R}}}{d\tilde{z}} = -\frac{f \cdot G \cdot \mu_g \cdot L}{\rho_g \cdot {d_p}^2} \cdot \frac{(1-\varepsilon)^2}{\varepsilon^3} \tag{13}$$

The friction factor f is evaluated by the well-known Ergun equation. In the molten salt shell and in the permeation zone, the pressure drop is neglected.

Boundary conditions

- Conditions on inlet section ($\tilde{z} = 0, \forall\tilde{r}$)

$$\tilde{u}_z\tilde{c}_{\text{CH}_4} = 1$$
$$\tilde{u}_z\tilde{c}_i = \frac{u_z c_i}{u_{z,0}c_{\text{CH}_4,0}} \quad (i = \text{H}_2\text{O}, \text{H}_2, \text{CO}, \text{CO}_2)$$
$$Y_{\text{H}_2} = 0 \quad \textit{Co-current configuration}$$
$$\tilde{T}_R = 1$$
$$\tilde{T}_P = \frac{T_{P,\text{in}}}{T_{R,\text{in}}} \quad \textit{Co-current configuration}$$
$$\tilde{T}_{\text{MS}} = \frac{T_{\text{MS,in}}}{T_{R,\text{in}}} \quad \textit{Co-current configuration}$$
$$P_R = P_{R,\text{in}}$$

- Conditions on reformer tube wall ($\tilde{r} = 1, \forall\tilde{z}$)

$$\frac{\partial(\tilde{u}_z\tilde{c}_i)}{\partial\tilde{r}} = 0$$
$$\lambda_{\text{er}}\frac{\partial\tilde{T}_R}{\partial\tilde{r}} = \frac{U \cdot R_i}{T_{R,\text{in}}}(T_{\text{MS}}(\tilde{z}) - T_{R|_{R_i}})$$

- Conditions on membrane tube radius ($\tilde{r} = r_{o,i}/r_{i,o}$, $\forall\tilde{z}$)

$$\frac{\partial(\tilde{u}_z\tilde{c}_i)}{\partial\tilde{r}} = 0 \quad (i = \text{CH}_4, \text{H}_2\text{O}, \text{CO}, \text{CO}_2)$$
$$\frac{d_p}{Pe_{\text{mr}}} \cdot \frac{u_{z,0}c_{\text{CH}_4,0}}{r_{i,0}}\frac{\partial(\tilde{u}_z\tilde{c}_{\text{H}_2})}{\partial\tilde{r}} = N^m_{\text{H}_2}$$
$$\frac{\lambda_{\text{er}}}{r_{i,0}} \cdot \frac{\partial\tilde{T}_R}{\partial\tilde{r}} = U_1 \cdot (\tilde{T}_{R|r_{o,i}} - \tilde{T}_P)$$

Numerical solution

In order to solve the set of partial differential equations, the radial coordinate is discretised by means of central second-order differences. An ODE set is obtained and solved by the Runge–Kutta method.

The reactor performance is evaluated through the following quantities:

$$X_{\text{CH}_4} = \frac{F_{\text{CH}_4,\text{in}} - F_{\text{CH}_4,\text{out}}}{F_{\text{CH}_4,\text{in}}} \quad \text{methane conversion}$$

$$X_{\text{CO}_2} = \frac{F_{\text{CO}_2,\text{out}} - F_{\text{CO}_2,\text{in}}}{F_{\text{CH}_4,\text{in}}} \quad \text{carbon dioxide yield}$$

$$Y_{\text{H}_2} = \frac{F_{\text{H}_2,\text{perm,out}}}{F_{\text{CH}_4,\text{in}}} \quad \text{hydrogen recovered per mole of methane}$$

DOI: 10.1002/apj

Table 1. Reformers dimensions imposed in the simulations.

Reactor length (L)	External radius of outer tube ($r_{o,o}$)	Internal radius of outer tube ($r_{i,o}$)	External radius of membrane tube ($r_{o,i}$)	Internal radius of membrane tube ($r_{i,i}$)
10 m	9.84 cm	8.57 cm	5.08 cm	3.81 cm

RESULTS AND DISCUSSION

Simulations have been carried out by imposing the reformer dimensions reported in Table 1.

Each reformer volume is calculated so that the total catalyst mass is equal to the one typically used in traditional reformers (tube diameter 0.126 m, length 12 m, void bed fraction $\varepsilon \cong 0.5$,).[1]

Table 2 reports the operating conditions imposed. The value of catalyst bed density has been imposed as being equal to 1016 kg/m^3 and the pellets equivalent diameter is 0.011 m.[1] The pseudo-effectiveness factor has been imposed equal to 0.02, according to the average value reported by Xu and Froment[20]

The value of the mass flow rate of molten salt in the reactor system shell is an average value for a single module of CSP plant, composed by a 1200-m-long streak, which globally occupies 1.5 ha.[21]

Table 2. Operating conditions.

$T_{R,\text{in}}$	$T_{P,\text{in}}$	$T_{\text{MS,in}}$	w_{MS}	P_P	$F_{\text{sweep}}/F_{\text{CH}_4,\text{in}}$
773 K	773 K	823 K	4 kg/s	1 bar	1

It is considered that the residual sensible heat of molten salt stream after chemical plant is used to generate electrical energy, with an efficiency of about 28%.

Effect of gas mixture residence time

The gas mixture residence time in the reformer is calculated according to

$$W/F = \frac{m_{\text{cat}}}{F_{\text{tot,in}}} \quad \frac{kg_{\text{cat}}}{\text{kmol}/h} \tag{14}$$

In Fig. 5, the effect of the residence time on methane conversion and on hydrogen recovered is reported.

An increasing residence time has a strong positive effect on the reactor performance. In fact, as the continuous hydrogen removal circumvents the equilibrium conditions in the MR, a longer residence time results in a larger fraction of hydrogen permeating through the membrane on the total hydrogen produced.

Therefore, benefits in integrating a Pd-based selective membrane in the reaction environment are more evident when longer residence times are adopted.

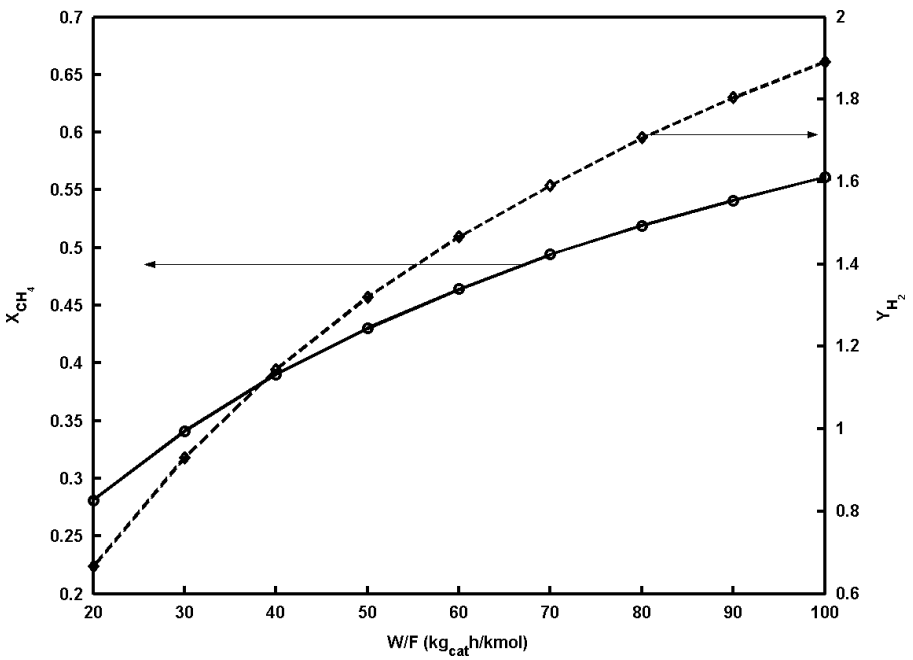

Figure 5. Effect of residence time on methane conversion and hydrogen recovered ($P_R = 10$ bar, steam-to-carbon ratio = 3).

DOI: 10.1002/apj

A longer residence time allows a greater recovery percentage of hydrogen in the permeation zone. In fact, the higher methane conversion obtained allows an increase in the permeation driving force as the hydrogen partial pressure difference between the reaction and permeation zone is higher [Eqn (6)]: the consequence is a positive effect on the membrane reformer performance also in terms of hydrogen recovery (about 60% at 20 $kg_{cat}h/kmol$ and 84.9% at 100 $kg_{cat}h/kmol$).

A comparison is also made with a traditional reactor. The traditional reactor has been simulated, nullifying the permeation flux in Eqn (6) and the global heat transfer coefficient between the reaction and permeation zone in Eqn. (9). If the membrane is not assembled in the reaction environment, the molten salt stream at 550 °C is not able to supply the heat required for satisfactory reaction advancement: methane conversion obtained in the traditional reactor is 0.2 at 20 $kg_{cat}h/kmol$, 0.232 at 60 $kg_{cat}h/kmol$ and 0.243 at 100 $kg_{cat}h/kmol$. A worthy assessment is that the benefits in the integration of a Pd-based selective membrane in the reaction environment are crucial and better when longer residence times are adopted.

Figure 6 reports the total pure hydrogen recovered in the outlet of the permeation zone and the electric power generated by the residual sensible heat of molten salt stream by imposing the four tubes-and-shell configuration (Fig. 4). When residence time increases, for a fixed reactor size, the total hydrogen produced is reduced because the methane feedstock is reduced as well. This means that a lower amount of methane is fed to the reactor and, although it reacts better, the total hydrogen produced and recovered is lower. On the other hand, the electricity produced is greater, owing to the lower heat duty required by the reactions that leads to a greater molten salt temperature at the outlet of chemical plant (493.5 °C at 20 $kg_{cat}h/kmol$ *vs* 525 °C at 100 $kg_{cat}h/kmol$).

Effect of pressure and steam-to-carbon ratio

In the following, the effects of the reaction zone pressure and the steam-to-carbon ratio on the solar membrane reformer performance are reported.

The operating pressure has two contrasting effects on the membrane reformer behaviour:

- a negative thermodynamics effect as reactions (1) and (3) occur with a reduction in the gas volume and
- a positive permeation effect as increasing the reaction zone pressure leads to a stronger permeation driving force [Eqn (6)]

The steam-to-carbon ratio also has a double effect:

- a positive thermodynamics effect and
- a negative permeation effect because increasing the quantity of steam supplied reduces the hydrogen partial pressure in the reaction zone, and consequently the permeation driving force becomes lower [Eqn (6)]

Figures 7 and 8 report methane conversion and hydrogen yield (Y_{H2}) at various operating pressure and steam-to-carbon ratio. Both operating conditions have positive

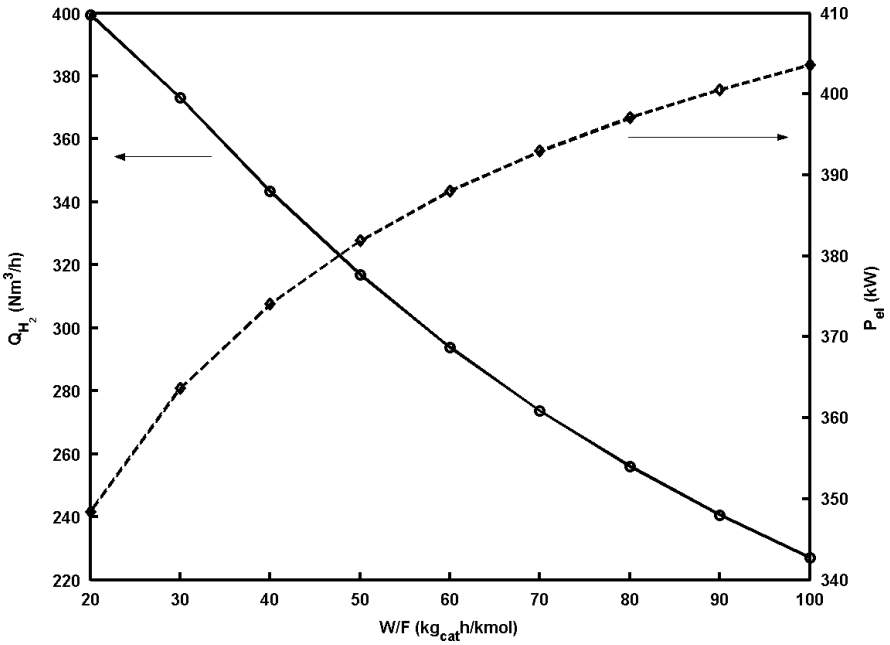

Figure 6. Total hydrogen permeated and electric power produced by residual molten salt sensible heat.

DOI: 10.1002/apj

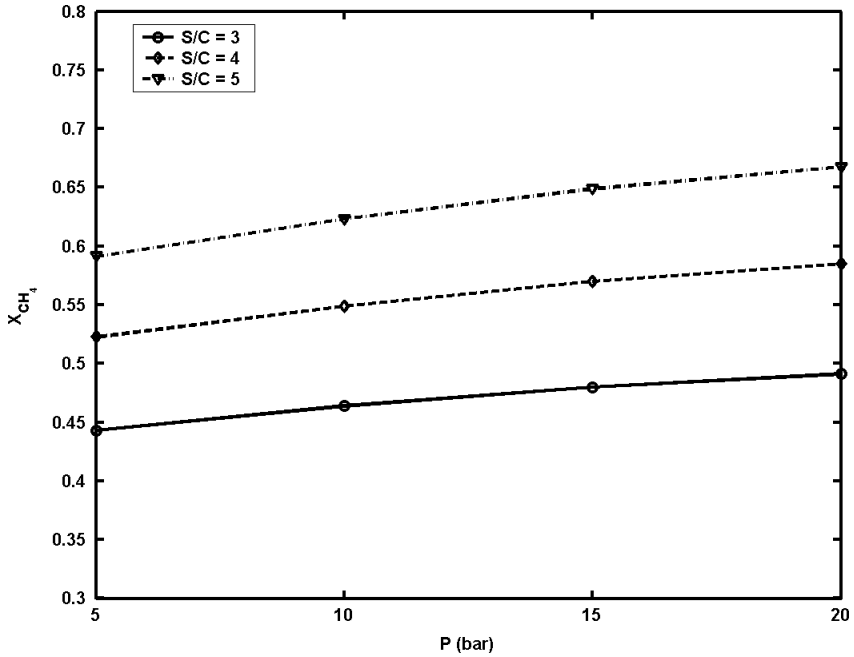

Figure 7. Methane conversion *vs* reaction pressure at various steam-to-carbon ratio (W/F = 60 kg_{cat}h/kmol).

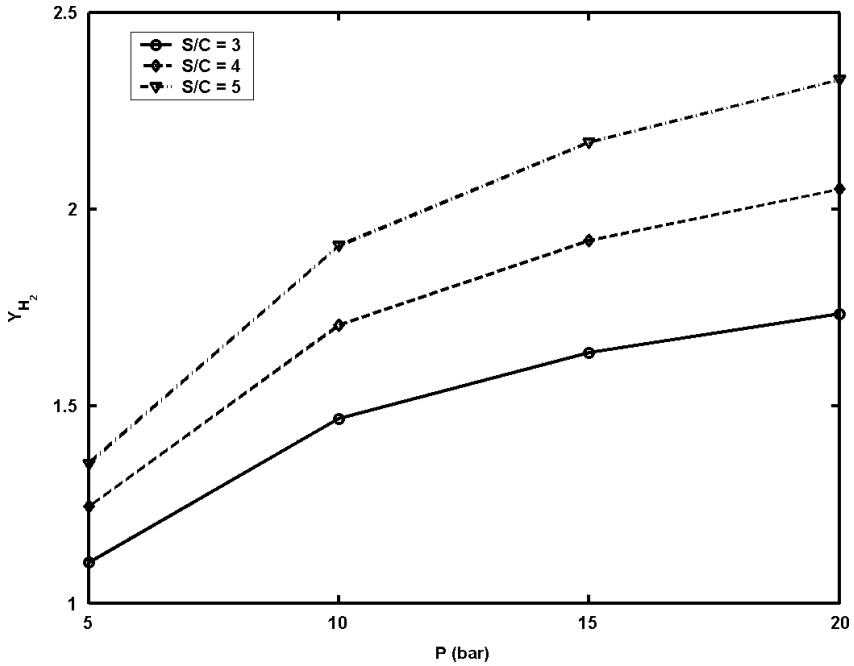

Figure 8. Hydrogen recovered *vs* reaction pressure at various steam-to-carbon ratios (W/F = 60 kg_{cat}h/kmol).

effects on reactor performance in terms of reaction and permeation advancement.

Regarding the reaction pressure, the positive effect on the permeation flux is stronger than the negative one on reaction thermodynamics: in fact, globally, the methane conversion increases at higher pressure. Obviously, the Y_{H2} also increases.

The steam-to-carbon ratio also has a positive effect on the reactor behaviour. This is due probably to the fact that increasing the steam-to-carbon ratio leads to a strong effect on conversion of reactions (Fig. 7) and this leads to an increase in the hydrogen partial pressure, although more quantity of steam is required in the reaction environment.

DOI: 10.1002/apj

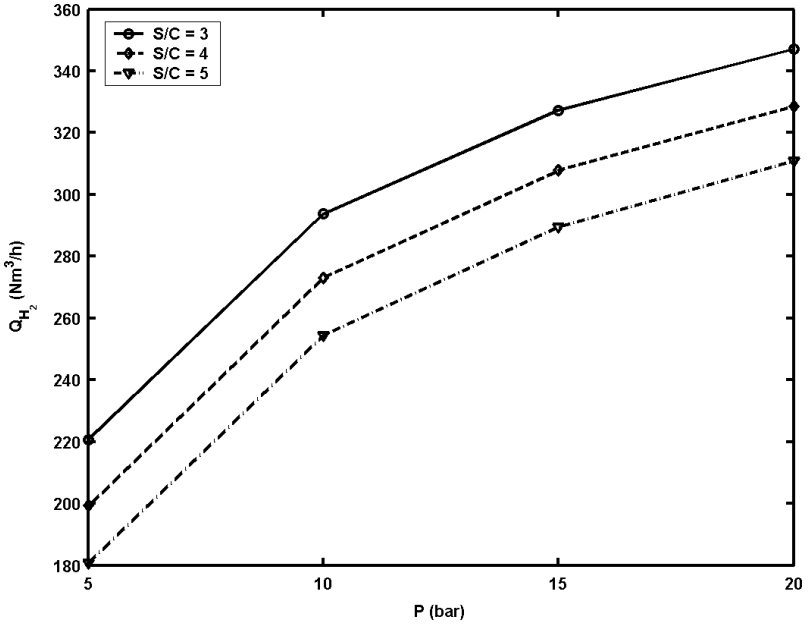

Figure 9. Total hydrogen permeated *vs* operating pressure and steam-to-carbon ratio (W/F = 60 kg_{cat}h/kmol).

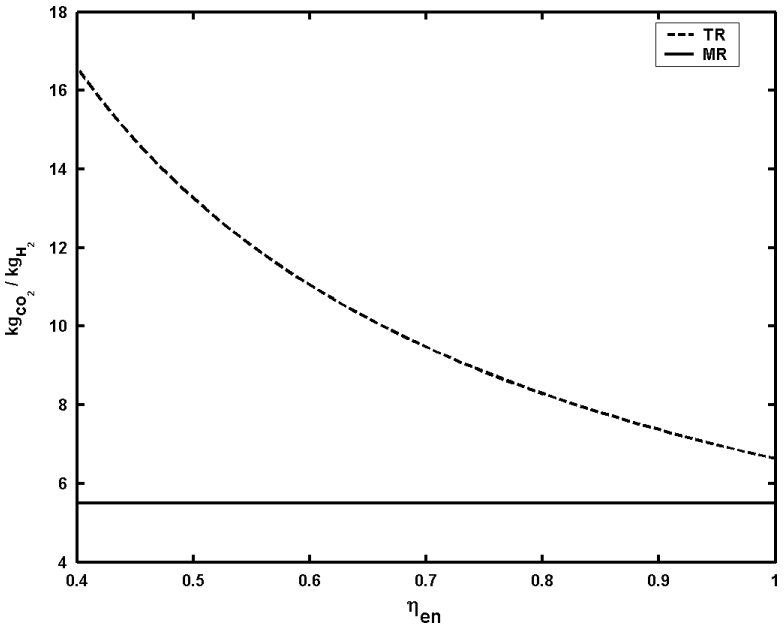

Figure 10. CO_2 emissions for unit of hydrogen produced for traditional process and for the innovative process proposed.

Figure 9 reports the total hydrogen permeated and recovered from the reactors system. It has to be noted that it increases with pressure but decreases when the steam-to-carbon ratio is higher. This can be explained considering that increasing the steam-to-carbon ratio, at fixed residence time and therefore the total inlet molar flow rate, leads to the reduction in methane feedstock, which reacts better but globally produces a lower amount of hydrogen.

The electric power produced by the system is almost constant in the pressure and steam-to-carbon ranges simulated, varying within 386.4–394.3 kW.

Reduction of GHG emissions

The measurement of CO_2 emissions reduction integrating the selective membrane in the solar reforming

DOI: 10.1002/apj

reactors is evaluated. The calculation of the total CO_2 emitted by the steam-reforming process can be done considering the energy efficiency of the process, defined as

$$\eta_{en} = \frac{LHV_{H_2}}{n_{CH_4} \cdot LHV_{CH_4}} \quad (15)$$

where LHV_{H_2} and LHV_{CH_4} are the lower heating value of hydrogen and methane respectively and nCH_4 are the overall moles of methane required to produce a mole of hydrogen both as reagent and fuel burned to supply thermal needs in the traditional process.

From Eqn (15):

$$n_{CH_4} = n_{CO_2} = \frac{LHV_{H_2}}{\eta_{en} \cdot LHV_{CH_4}} \quad (16)$$

For the solar reformer, the heat duty is supplied by the solar energy source, which is completely CO_2 free. Therefore, the greenhouse gas emissions are exclusively due to the methane conversion.

To produce 1 mol of hydrogen, 1/4 mol of methane is needed [Eqn (3)] and consequently:

$$n_{CO_2} = 0.25 \frac{mol_{CO_2}}{mol_{H_2}} = 5.5 \frac{kg_{CO_2}}{kg_{H_2}} \quad (17)$$

A mass of 5.5 kg of CO_2 is emitted per kilogram of H_2 produced, regardless of the energy efficiency.

In Fig. 10, a comparison is made between the greenhouse gas emissions resulting from the traditional process and those from the MR technology on the basis of the traditional process efficiency, characterised by a total efficiency within the range 45–80%.

The integration of the Pd-based membranes and use of solar energy for process heat duty allow a CO_2 emission reduction of 33–67%.

CONCLUSIONS

An innovative plant for the production of hydrogen consisting of the harmony between the integration of the H_2-selective membrane directly inside the reaction environment, allowing the reduction of operating temperature required for reaction conversion enhancement, and the CSP technology that uses molten salt stream as heat carrier, has been proposed.

The exhaustive MR modelling allows the evaluation of the plant performance, in terms of hydrogen produced and separated and of electric power produced by the residual molten salt sensible heat. Results attest the goodness of the technology as satisfactory methane conversions are obtained (up to 67%) using a clean energy source and consequently reducing the GHG emissions of the steam-reforming process.

In conclusion, the process layout proposed can give a crucial contribution towards a more sustainable way for producing large amounts of hydrogen and reaching the Kyoto protocol objectives.

Acknowledgements

The authors are grateful to Prof. L. Marrelli of University of Rome 'La Sapienza' for useful discussions and contributions, and to A. Giaconia, P. Tarquini, G. Caputo and R. Grena of ENEA-Casaccia for the contributions about CSP technology.

NOMENCLATURE

B_H	Hydrogen permeability, $\frac{kmol}{m \times h \times kPa^{0.5}}$
$F_{CH_4,in}$	Inlet methane flow rate, kmol/h
$F_{CH_4,out}$	Outlet methane flow rate, kmol/h
$F_{CO_2,in}$	Inlet carbon dioxide flow rate, kmol/h
$F_{CO_2,out}$	Outlet carbon dioxide flow rate, kmol/h
$F_{H_2,perm}$	Hydrogen flow rate in permeation zone, kmol/h
$F_{H_2,perm,out}$	Outlet hydrogen flow rate in permeation zone, kmol/h
$F_{p,tot}$	Total permeation zone molar flow rate, kmol/h
F_{sweep}	Sweeping gas flow rate in permeation zone, kmol/h
$F_{tot,in}$	Total inlet molar flow rate, kmol/h
G	Mass specific gas flow rate, $\frac{kg}{m^2 \times h}$
$(-\Delta H_j)$	j-th reaction enthalpy, kJ/kmol
L	Reactor length, m
LHV_{CH_4}	Methane lower heating value, kJ/kmol
LHV_{H_2}	Hydrogen lower heating value, kJ/kmol
$N_{H_2}^m$	Hydrogen flux permeating through membrane, $\frac{kmol}{m^2 \times h}$
P_{el}	Electric power produced, kW
Pe_{mr}	Mass effective radial Peclet number
P_P	Permeation zone pressure, kPa
P_R	Reaction zone pressure, kPa
Pr	Prandtl number
Q_{H_2}	Hydrogen produced volume flow rate, $\frac{Nm^3}{h}$
R_j	Kinetic rate of j-th reaction, $\frac{kmol}{kg_{cat} \times h}$
Re	Reynolds number (Gd_p/μ_g)
$\tilde{T}_{MS}$	Dimensionless molten salt temperature
$\tilde{T}_P$	Dimensionless permeation zone temperature
$T_{P,in}$	Inlet permeation zone temperature, K
$\tilde{T}_R$	Dimensionless reaction zone temperature
$T_{R,in}$	Inlet reaction zone temperature, K
U	Overall heat transfer coefficient between outside and reaction zone, $\frac{kJ}{m^2 \times h \times K}$

U_1 Overall heat transfer coefficient between reaction and permeation zone, $\frac{\text{kJ}}{\text{m}^2 \times \text{h} \times \text{K}}$

W/F Gas mixture residence time, $\frac{\text{kg}_{\text{cat}}}{\text{kmol/h}}$

X_{CH_4} Methane conversion

X_{CO_2} Carbon dioxide yield

Y_{H_2} Hydrogen recovered per mole of methane

$\tilde{c}_i$ Dimensioless molar concentration, i = CH_4, H_2O, H_2, CO, CO_2

$c_{i,\text{in}}$ Inlet molar concentration, kmol/m^3, i = CH_4, H_2O, H_2, CO, CO_2

$c_{p,m}$ Gas mixture specific heat, $\frac{\text{kJ}}{\text{kmol} \times \text{K}}$

$c_{p,\text{MS}}$ Molten salt specific heat, $\frac{\text{kJ}}{\text{kmol} \times \text{K}}$

$c_{p,\text{perm}}$ Gas mixture specific heat in permeation zone, $\frac{\text{kJ}}{\text{kmol} \times \text{K}}$

c_{tot} Total molar concentration, kmol/m^3

d_p Equivalent particle diameter, m

f Friction factor

h_{P,H_2} Permeation zone hydrogen enthalpy, kJ/kmol

h_{R,H_2} Reaction zone hydrogen enthalpy, kJ/kmol

h_W Heat transport coefficient near wall, $\frac{\text{kJ}}{\text{m}^2 \times \text{h} \times \text{K}}$

$h_{w,p}$ Forced convection heat transport coefficient in permeation zone, $\frac{\text{kJ}}{m^2 \cdot h \cdot K}$

m_{cat} Catalyst mass, kg

$p_{\text{H}_2,\text{perm}}$ Hydrogen partial pressure in permeation zone, kPa

$p_{\text{H}_2,\text{reac}}$ Hydrogen partial pressure in reaction zone, kPa

$r_{i,i}$ Internal tube internal radius, m

$r_{o,i}$ Internal tube external radius, m

$r_{i,o}$ External tube internal radius, m

$r_{o,o}$ External tube external radius, m

$\tilde{r}$ Dimensionless radial coordinate

$\tilde{u}_z$ Dimensionless gas velocity

$u_{z,in}$ Inlet gas velocity, m/h

w_{MS} Molten salt mass flow rate, kg/h

$\tilde{z}$ Dimensionless axial coordinate

Greek letter

α_{mem} Membrane thermal conductivity, $\frac{\text{kJ}}{\text{m} \times \text{h} \times \text{K}}$

α_{met} Metal conductivity, $\frac{\text{kJ}}{\text{m}^2 \times \text{h} \times \text{K}}$

δ Membrane thickness, m

ε Void fraction

η_{en} Process energy efficiency

η_j Effectiveness factor of j-th reaction

λ_{er} Effective radial thermal conductivity, $\frac{\text{kJ}}{\text{m} \times \text{h} \times \text{K}}$

λ_g Gas phase thermal conductivity, $\frac{\text{kJ}}{\text{m} \times \text{h} \times \text{K}}$

μ_g Gas mixture viscosity, $\frac{\text{kg}}{\text{m} \times \text{h}}$

ρ_b Packed bed density, kg/m^3

ρ_g Gas mixture density, kg/m^3

REFERENCES

[1] S. Elnashaie, S. Elshishini. *Modelling, Simulation and Optimization of Industrial Fixed Bed Catalytic Reactors*, *Topics in Chemical Engineering*, Vol. 7, Gordon and Breach Science Publisher: USA, **1993**.

[2] J. Shu, B. Grandjean, S. Kaliaguine. *Appl. Catal. A: Gen.,* **1994;** *119*, 305–325.

[3] Y. Lin, S. Liu, C. Chuang, Y. Chu. *Catal. Today,* **2003;** *82*, 127–139.

[4] F. Gallucci, L. Paturzo, A. Basile. *Int J. Hydrogen Energy,* **2004;** *29*, 611–617.

[5] J. Oklany, K. Hou, R. Hughes. *Appl. Catal. A: Gen.,* **1998;** *170*, 13–22.

[6] G. Madia, G. Barbieri, E. Drioli. *Can. J. Chem. Eng.,* **1999;** *77*, 698–706.

[7] W. Yu, T. Ohmori, T. Yamamoto, E. Endo, T. Nakaiwa, T. Hayakawa, N. Itoh. *Int. J. Hydrogen Energy,* **2005;** *30*, 1071–1079.

[8] M. Chai, M. Machida, K. Eguchi, H. Arai. *Appl. Catal. A: Gen.,* **1994;** *110*, 239–250.

[9] F. Fernandez,A. Soares Jr. *Fuel,* **2006;** *85*, 569–573.

[10] M. Koukou, N. Papayannakos,N.C. Markatos. *Chem. Eng. J.,* **2001;** *83*, 95–105.

[11] C. Fukuhara, A. Igarashi. *J. Chem. Eng. Jpn.,* **2003;** *36*(5), 530–539.

[12] M. De Falco, L. Di Paola, L. Marrelli, P. Nardella. *Chem. Eng. J.,* **2007;** *128*, 115–125.

[13] F. Gallucci, M. De Falco, S. Tosti, L. Marrelli, A. Basile. *Int. J. Hydrogen Energy,* **2007;** *32*, 4052–4058.

[14] F. Gallucci, M. De Falco, S. Tosti, L. Marrelli, A. Basile. *Int. J. Hydrogen Energy,* **2008;** *33*, 644–651.

[15] M. De Falco, P. Nardella, L. Marrelli, L. Di Paola, A. Basile, F. Gallucci. *Chem. Eng. J.,* **2008;** *138*(1–3), 442–451.

[16] J. Xu,G. Froment. *AIChE J.,* **1989;** *35*(1), 88–96.

[17] B.D. Kulkarni,L.K. Doraiswamy. *Catal. Rev.: Sci. Eng.,* **1980;** *22*(3), 431–483.

[18] E. Tsotsas, E. Schlü nder. *Chem. Eng. Sci.,* **1990;** *45*, 819–837.

[19] C. Li, B. Finlayson. *Chem. Eng. Sci.,* **1977;** *32*, 1055–1066.

[20] J. Xu,G. Froment. *AIChE J.,* **1989;** *35*(1), 97–103.

[21] M. De Falco, A. Giaconia, L. Marrelli, P. Tarquini, R. Grena, G. Caputo, *Int. J. Hydrogen Energy,* **2009;** *34*, 98–109.